Transient Harman Measurement of the Cross-plane ZT of InGaAs/InGaAlAs Superlattices with Embedded ErAs Nanoparticles

Rajeev Singh, Zhixi Bian, Gehong Zeng[1], Joshua Zide[1], James Christofferson, Hsu-Feng Chou[1], Art Gossard[1], John Bowers[1], and Ali Shakouri
Electrical Engineering Department, University of California
Santa Cruz, CA 95064, U.S.A.
[1]Department of Electrical and Computer Engineering, University of California
Santa Barbara, CA 93106, U.S.A.

ABSTRACT

The transient Harman technique is used to characterize the cross-plane *ZT* of InGaAs/InGaAlAs superlattice structures with embedded ErAs nanoparticles in the well layers. ErAs nanoparticles have proven to substantially reduce the thermal conductivity while slightly increasing the electrical conductivity of bulk InGaAs. The InGaAs/InGaAlAs superlattice structure was designed to have a barrier height of approximately 200meV. Although ErAs nanoparticles provide free carriers inside the semiconductor matrix, additional doping with Si increased the Fermi energy to just below the barrier height. The bipolar transient Harman technique was used to measure device *ZT* of samples with different superlattice thicknesses in order to extract the intrinsic cross-plane *ZT* of the superlattice by eliminating the effects of device Joule heating and parasitics. High-speed packaging is used to reduce signal ringing due to electrical impedance mismatch and achieve a short time resolution of roughly 100ns in transient Seebeck voltage measurement. The measured intrinsic cross-plane *ZT* of the superlattice structure is 0.13 at room temperature. This value agrees with calculations based on the Boltzmann transport equation and direct measurements of specific film properties. Theoretical calculations predict cross-plane *ZT* of the superlattice to be greater than 1 at temperatures greater than 700K.

INTRODUCTION

Thin-film semiconducting materials are receiving great interest for use in thermoelectric devices due to the ability to enhance the Seebeck coefficient (S) and reduce the thermal conductivity (κ) of the films by utilizing nanostructures. In particular, superlattice structures are being studied to achieve larger material S and lower κ without significantly reducing the electrical conductivity (σ) of the material. These factors impact thermoelectric material figure-of-merit (ZT) given by

$$ZT = \frac{S^2 \sigma}{\kappa} T \,, \tag{1}$$

where T is the ambient temperature. By utilizing tall barriers and large well dopant concentrations that place the Fermi level (E_f) within a thermal energy (kT) below the barrier, material σ can be maintained while increasing material S through the enhancement of differential conductivity $\sigma(E)$ via electron filtering [1-3]. In addition, material κ in superlattice structures can be reduced by interfacial phonon scattering [4,5]. Embedded metallic nanoparticles in the

superlattice well regions can further increase phonon scattering in the material while providing additional free carriers [6-8].

Experimental measurement of cross-plane characteristics of superlattice structures can be difficult due to device parasitics that are often difficult to account for. The direct cross-plane *ZT* measurement of thin-film superlattices is challenging due to the microsecond-scale response time of the devices as well as the small relative magnitudes of film properties to device parasitics. We have utilized the bipolar transient Harman method on devices of different superlattice thicknesses to extract the intrinsic cross-plane *ZT* of InGaAs/InGaAlAs superlattices with ErAs nanoparticles embedded in the well layers. A bipolar measurement method is used to eliminate the effects of Joule heating in the device while the measurement of devices with different superlattice thicknesses is utilized to extract the intrinsic *ZT* of the thin-film superlattice independent of device parasitics [9,10].

THEORY

The transient Harman method utilizes an applied electrical current (I) to create a temperature gradient (ΔT) in a thermoelectric device that is due to both Joule and Peltier effects. The total steady-state voltage (V_T) developed across a thermoelectric device due to an applied current is composed of a component due to the device's total electrical resistance (V_R) and a Seebeck voltage component (V_S) proportional to the temperature difference across the device. In the event that I is terminated, V_R will vanish "instantaneously" while V_S decays more slowly as the device returns to thermal equilibrium. To determine the component of V_S generated due to the Peltier effect alone, the fact that the polarity of the component of V_S due to the Peltier effect (V_{SP}) changes with the direction of I while the polarity of the Seebeck voltage component due to the Joule effect (V_{SJ}) is independent of the direction of I is exploited. The Peltier component of V_S is given by

$$V_{SP} = \frac{V_S(+I) - V_S(-I)}{2}. \tag{2}$$

The measured Seebeck and electrical voltages correspond to the complete thermoelectric devices. One can extract the intrinsic *ZT* of a thin-film material using a variable film thickness approach. The thin-film *ZT* is given by

$$ZT_{Film} = \frac{\partial V_{SP} / \partial l}{\partial V_R / \partial l}, \tag{3}$$

where l is the film thickness. The bipolar transient Harman technique is used to extract V_{SP} and V_R of the entire device for a given I. By inspecting the electro-thermal circuits of devices of different film thicknesses and deriving the change of electrical and Seebeck voltages when the thickness varies from l_1 to l_2, equation 3 can be written as

$$ZT_{Film} = \frac{\Delta V_{sp}(l_1 \to l_2)}{\Delta V_R(l_1 \to l_2)} = \frac{\dfrac{S_{Film}^2 TI}{\kappa_{Film}} \dfrac{l_2 - l_1}{A_{Film}}}{I\rho_{Film} \dfrac{l_2 - l_1}{A_{Film}}} = \frac{S_{Film}^2 \sigma_{Film} T}{\kappa_{Film}}. \tag{4}$$

All device parasitics due to the substrate, buffer layers, and electrical contacts have cancelled in equation 4 and only the intrinsic *ZT* of the thin-film material remains.

EXPERIMENT

N-type InGaAlAs superlattice structures were grown lattice-matched to n-type InP substrate using molecular beam epitaxy (MBE). The 10nm-thick barrier regions were grown as a digital alloy of $(InGaAs)_{0.6}(InAlAs)_{0.4}$ and not intentionally doped. The 20nm-thick InGaAs wells were deposited along with a very small fraction of Er to a composition of $InGaAs_{0.997}Er_{0.003}$. This resulted in the formation of randomly distributed ErAs nanoparticles in the wells. Although the ErAs nanoparticles contribute free carriers, the well regions were co-doped with silicon to a final carrier concentration of $10^{19}cm^{-3}$ [7, 8].

The key to making a variable thickness measurement accurate is for all device parameters other than the film thickness to remain constant. In this regard, devices of different film thicknesses were fabricated by etching the same film to various depths. Device fabrication steps were performed simultaneously on a film that was etched down to 2.5 and 5.7μm. It is therefore assumed that fabrication consistency was achieved. Device mesas of different areas were etched down by 1μm in order to define electrical current in the film to approximately the device cross-section. SiN_x electrical insulating layers and Au device side contacts were subsequently deposited on the etched film. The InP substrate was lapped down to 200μm in an effort to reduce its parasitic contributions of electrical and thermal resistance before backside ground contact metallization. Figure 1 is a side-view schematic of the variable film thickness devices while figure 2 is a top-view image of the fabricated devices.

In order for the transient Harman method to be accurate, the following experimental conditions must be achieved: device adiabaticity and a maximum steady-state temperature gradient for a given *I*. For large *ZT* materials that are able to create large temperature gradients, the temperature dependence of thermoelectric properties can become an important consideration as the average temperature of a heat-sinked thermoelectric device can change dramatically with the direction of *I*. In this case, the use of the smallest *I* possible to achieve decent signal magnitudes in transient voltage measurement will result in a lower device ΔT and therefore reduce the effect of a large temperature dependence on the measurement accuracy.

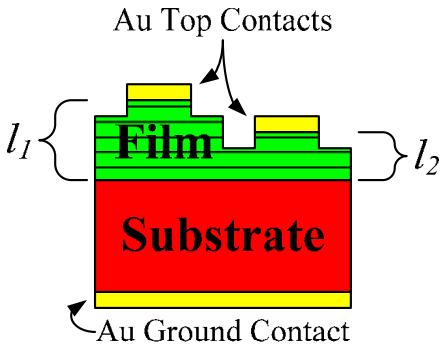

Figure 1. Side-view diagram of variable film thickness devices

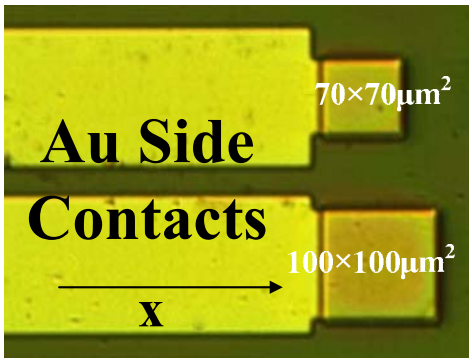

Figure 2. Top-view image of fabricated thin-film devices

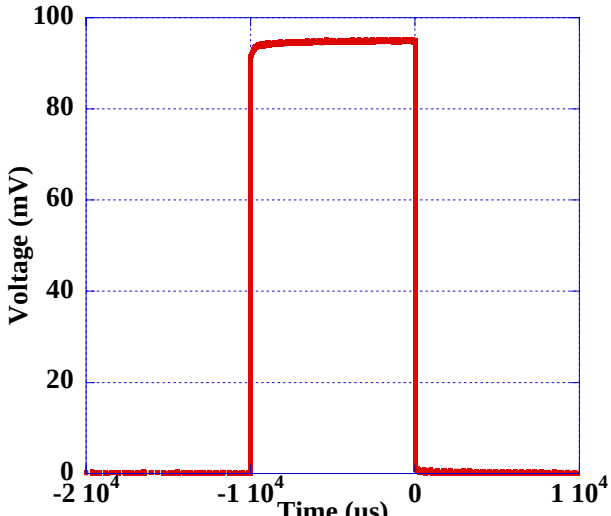

Figure 3. V_T vs. t at I = 400mA (5.7μm-thick film, 70×70μm^2 mesa)

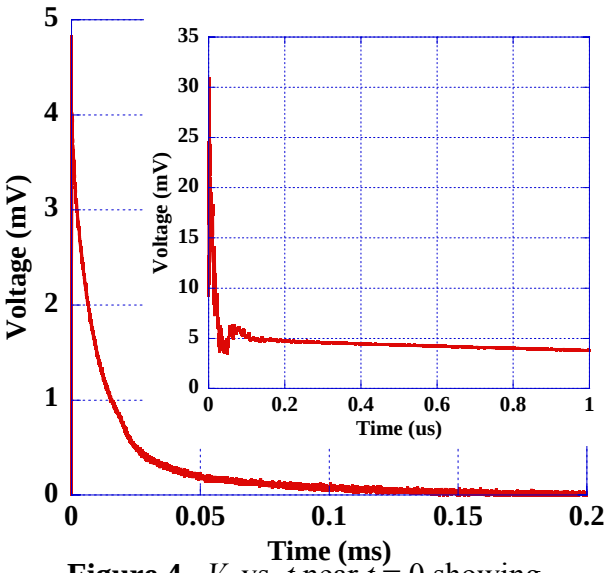

Figure 4. V_S vs. t near t = 0 showing transient decay and resolution of ~ 100ns

The wafer containing the fabricated devices of different thicknesses was mounted in a relatively massive high-speed copper device package with indium solder. Two different device mesa areas (70×70μm^2 and 100×100μm^2) were tested to determine any size-dependence of measured *ZT* that may result from non-adiabatic device conditions due to thermal leakage through the electrical side contact. Four-wire electrical connections to the devices were utilized to inject current and measure resulting voltages directly across the device. Measurement of V_R at either pulse edge was used to determine the electrical resistance of the devices. This high-speed pulse edge measurement ensures that generated thermoelectric voltages do not cause an error in device resistance measurement. Figure 3 above is a plot of V_T versus time during a current pulse of 400mA through a device consisting of a 5.7μm-thick film whose mesa area is 70×70μm^2. The temporal resolution of device V_S measurement achieved is roughly 100ns after the falling edge of the current pulse. Figure 4 above shows the time resolution achieved for V_S in the measurements. Extrapolation of curve fits was used to determine the value of V_S at the falling edge (*t=0*).

RESULTS

Figure 5 below is a plot of device V_{SP} and V_R versus I for two film thicknesses and mesa areas. It is apparent that V_{SP} is linearly proportional to I. The large V_R relative to V_{SP} was found to be mainly due to the resistance of the device side contact. Figure 6 below is a plot of the extracted intrinsic cross-plane *ZT* of the InGaAs/InGaAlAs:ErAs superlattice material and the *ZT* of the four devices tested. The intrinsic cross-plane *ZT* extracted from the 100×100μm^2 devices is 0.13 ±0.01 while the value extracted from the 70×70μm^2 devices is 0.08 ±0.01. This size-dependence is thought to be mainly due to thermal leakage from the top of the device mesa through the side electrical contact that creates a non-uniform temperature distribution on the mesa. The surface temperature uniformity should decrease with decreasing mesa area. Calculations based upon the Boltzmann transport equation predict a *ZT* of 0.12 to 0.15 at room temperature [8].

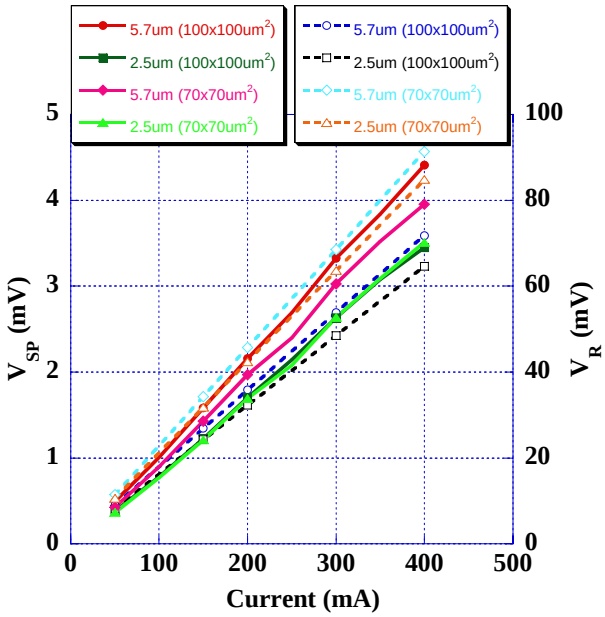

Figure 5. Device V_{SP} (solid) and V_R (dashed) vs. I

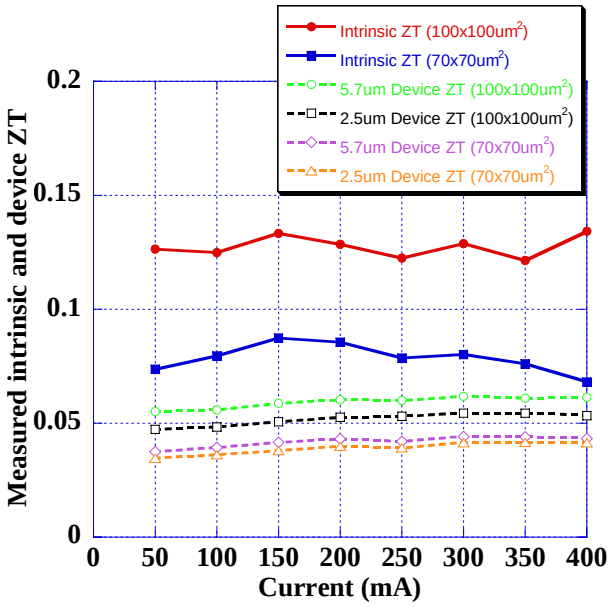

Figure 6. Intrinsic (solid) and device (dashed) ZT vs. I

Thermoreflectance imaging of the mesas of different area confirms that mesa surface temperature non-uniformity is significant on the 70×70μm^2 device mesa while the 100×100μm^2 device mesa was found to have a relatively uniform temperature profile. Figure 7 is a thermoreflectance (ΔR/R) line-scan along the x-direction (see Figure 2) from the side contact region across the device mesa and extending into the SiN_x insulating layer. The device was modulated with a sinusoidal current of approximately 400mA peak-to-peak at 750Hz. The thermoreflectance system was configured to lock-in to the signal's first harmonic. Therefore, the line scan reflects the temperature profile as a result of the Peltier effect in the device. This measurement of the temperature distribution due to the Peltier effect alone corresponds to the quantity used to determinine device *ZT*. This result can explain the dependence of intrinsic *ZT* on the mesa area of the device that the value is extracted from.

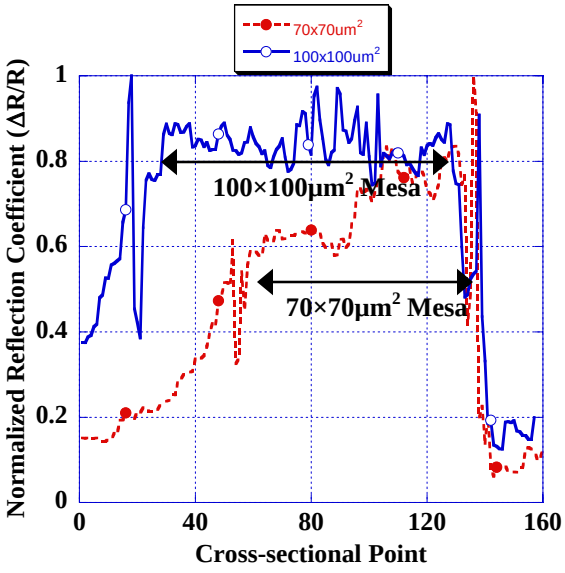

Figure 7. Cross-sectional line-scan of ΔR/R vs. x for 70×70μm^2 and 100×100μm^2 device mesas showing increased temperature uniformity on the larger area mesa

CONCLUSIONS

We have utilized the transient Harman method on variable thickness InGaAs/InGaAlAs thin-film superlattice-based thermoelectric devices with ErAs nanoparticles randomly distributed in the wells to extract the intrinsic cross-plane *ZT* of the film. Due to the device area dependence of the *ZT* values measured, it appears that the devices are not entirely under adiabatic conditions in the experiment and that this non-adiabaticity increases as device area decreases. Thermal imaging of device mesas of different areas has confirmed thermal leakage through the electrical side contact. The temperature non-uniformity appears to have a large effect on the measured value of *ZT*. The temperature distribution on the $100\times100\mu m^2$ device mesa is quite uniform, and from this size we have extracted an intrinsic cross-plane thin-film *ZT* of 0.13.

Future work will be dedicated to improving the design of the devices used for this measurement in order to meet the adiabatic requirements of the transient Harman method. Specifically, device electrical side contact geometry has shown to have a great affect on the thermal load on the device mesa. In addition, a high-temperature vacuum chamber capable of high-speed transient measurements will be designed and fabricated to measure the *ZT* of novel nanostructured thermoelectric materials above room temperature.

ACKNOLEDGEMENTS

This work is supported by the Office of Naval Research (ONR) - Multidisciplinary University Research Initiative (MURI) grant: Thermionic Energy Conversion Center.

REFERENCES

1. A. Shakouri and J. Bowers, Appl. Phys. Lett. **71**, 1234 (1997).
2. G. D. Mahan, and L. M. Woods, Phys. Rev. Lett. **80**, 4016 (1998).
3. D. Vashaee and A. Shakouri, Phys. Rev. Lett. **92**, 106103 (2004)
4. G. Chen, and A. Shakouri, *Transactions of the ASME. Journal of Heat Transfer*, **124,** 242 (2002).
5. S. T. Huxtable, A. R. Abramson, C. L. Tien, A. Majumder, C. Labounty, X. Fan, G. Zeng, J. E. Bowers, A. Shakouri, and E. T. Croke, Appl. Phys. Lett. **80,** 1737 (2002).
6. W. Kim, S. Singer, A. Majumdar, D. Vashaee, Zhixi Bian, A. Shakouri, G. Zeng, J. E. Bowers, J. M. Zide, and A. C. Gossard, Appl. Phys. Lett., Low thermal conductivity and high Seebeck coefficient of superlattices, (*to be submitted*).
7. J. M. Zide, D. O. Klenov, S. Stemmer, A. C. Gossard, G. Zeng, J. E. Bowers, D. Vashaee and A. Shakouri, Appl. Phys. Lett. **87,** 112102 (2005).
8. J. M. Zide, D. Vashaee, G. Zeng, J. E. Bowers, A. Shakouri, and A. C. Gossard, Phys. Rev. Lett., Demonstration of electron filtering to increase the Seebeck coefficient in ErAs:InGaAs/InGaAlAs superlattices, (*submitted September 2005*).
9. Zhixi Bian, Y. Zhang, H. Schmidt, and A. Shakouri, *Proceedings of the 24th International Conference on Thermoelectrics*, *Clemson, 2005* (proceedings to be published).
10. R. Venkatasubramanian, E. Siivola, T. Colpitts, and B. O'Quinn, Nature (London) **413**, 597 (2001).